Effects of network robustness on explosive synchronization

Yang Liu[1,2] and Jürgen Kurths[1,3,4]
[1]*Potsdam Institute for Climate Impact Research, 14412 Potsdam, Germany*
[2]*Department of Computer Science, Technische Universität Berlin, 10587 Berlin, Germany*
[3]*Department of Physics, Humboldt University Berlin, 12489 Berlin, Germany*
[4]*Saratov State University, 410012 Saratov, Russia*

(Received 21 January 2019; revised manuscript received 11 June 2019; published 25 July 2019)

Current studies have shown that there is a positive correlation between the network assortativity and robustness and that the assortativity also plays an important role in explosive synchronization. In this paper, taking the network robustness as a global property, we investigate its significance as well as the influence of its interaction with the assortativity on explosive synchronization. Our numerical results demonstrate that explosive synchronization is suppressed in extreme situations of both the robustness and assortativity. In addition, through appropriate adjustments of them, a maximum hysteresis area between the forward and backward transitions can be reached. Furthermore, our results might also provide reference for those who are interested in effects of network structure on synchronization, though this problem is still challenging as we show in the discussion.

DOI: 10.1103/PhysRevE.100.012312

I. INTRODUCTION

Networks as an effective approach have widely been studied in numerous domains ranging from nonlinear science to biology and from statistical mechanics to medicine and engineering [1]. These studies are mainly twofold. On the one hand, a highly interacted system can be appropriately modeled by a graph whose nodes represent the dynamic units and whose edges capture their interactions. It is much easier to study the global properties of systems from a network perspective, such as the stability of power grids [2] or the spreading dynamics of messages or epidemics in communication systems [3]. On the other hand, studying the corresponding network provides rehearsal of manipulation on real systems and facilitates better solutions to control, predict, optimize, or reconstruct them [4,5]. In particular, synchronization on networks arouses much interest among scientists, because it may guide us to more profoundly understand the function and structure of real complex systems' dynamic processes [6,7], such as in power grids, climate systems, or neuron systems.

Recently, much attention has focused on a critical phenomenon, called explosive synchronization (ES) [7–10], which is observed when the coupled oscillators (e.g., of the Kuramoto system [11]) are associated with a scale-free topology [8]; i.e., the natural frequency of each oscillator proportionally corresponds to its number of connections, and they are coupled by the related adjacency matrix. Indeed, the node degree plays a crucial role in the ES phenomenon, not only of one node itself, but also of its neighbors. Thus, for example, the degree-degree correlation has been demonstrated to be important for the emergence of ES [12–15]. However, while studying the effects of network assortativity on ES, a fact which cannot be ignored is that there is also a strong association between the network assortativity and robustness [16,17].

In this paper, we view the network robustness $\mathcal{F}$ (see the next section for the mathematical definition) as a global attribute to capture the network structure and investigate its influence on ES, since network assortativity r is actually a local property. Following the assumption of Refs. [8,14], we mainly find that ES depends not only on the network assortativity but also on the network robustness. Specifically, there might exist a maximization of the hysteresis area which can be achieved by adjusting the network assortativity while keeping $\mathcal{F}$ constant. In particular, this process cannot be inverted, i.e., keeping the network assortativity in a certain status to adjust $\mathcal{F}$. In addition, we further discuss the response of $\mathcal{F}$ and r to the change of each other, which induces a gap between the enhancement and weakness. We also find that this gap actually plays an important role in ES.

II. MODEL

We consider a network $G(N, E)$ comprising $n = |N|$ nodes linked by $m = |E|$ edges where N and M are the node set and edge set, respectively. Then, for a certain $q = \ell/n$ where $\ell \in \mathbb{N}^+$ and $\ell \leqslant n$, the robustness of G against an intentional attack (remove the q-fraction hubs) [17] can be measured by the ratio between the size of the giant component $n_{\mathcal{G}}$ and the network size n, say, $\mathcal{G}(q) = n_{\mathcal{G}}/n$, which is associated with the assumption that the main part of a system still works even though some components failed [17]. In other words, a network with a larger $\mathcal{G}(q)$ means that it is more robust. However, there is a problem that a different q corresponds to a different $\mathcal{G}(q)$, which makes it difficult to compare the robustness among networks. Considering this, two types of metrics are developed: the critical threshold q_c [17,18],

$$q_c := \arg\min_{q_c \in \{q\}} \{q_c | \mathcal{G}(q > q_c) \sim 0, \forall q\}, \tag{1}$$

and the average giant fraction $\mathcal{F}$ [4],

$$\mathcal{F} := \frac{1}{n} \sum_q \mathcal{G}(q). \tag{2}$$

In this paper, we use $\mathcal{F}$ to measure the network robustness since it can more effectively capture the global change of the giant component instead of a special condition (q_c) where the giant component vanishes.

Letting $e_{ij} \in E$ correspond to a unique edge between nodes $i \in N$ and $j \in N$, we use the assortativity coefficient r in Ref. [16] to measure the network assortativity

$$r = \frac{\frac{1}{m}\sum_{e_{ij}\in E} k_i k_j - \left[\frac{1}{2m}\sum_{e_{ij}\in E}(k_i + k_j)\right]^2}{\frac{1}{2m}\sum_{e_{ij}\in E}\left(k_i^2 + k_j^2\right) - \left[\frac{1}{2m}\sum_{e_{ij}\in E}(k_i + k_j)\right]^2}, \tag{3}$$

in which k_i denotes the degree (the number of connections) of node i. Moreover, following the assumption of Ref. [8] viewing the dynamics of the nodes of G as phase oscillators coupled by the associated edges, we still employ the Kuramoto model [11] to govern the dynamics of the coupled oscillators:

$$\dot{\theta}_i = \omega_i + \lambda \sum_{j\in N} \mathcal{A}_{ij} \sin(\theta_j - \theta_i), \tag{4}$$

where $i \in N$, θ_i is the phase of oscillator i, and ω_i denotes the corresponding natural frequency. $\mathcal{A}_{ij}$ is a binary symbol; i.e., $\mathcal{A}_{ij} = 1$ if $e_{ij} \in E$, otherwise, $\mathcal{A}_{ij} = 0$. λ represents the coupling strength by adjusting the coherence (usually measured by the order parameter $\Re$) among the oscillators which will change:

$$\Re(t) e^{\mathrm{i}\psi(t)} = \frac{1}{n}\sum_{j\in N} e^{\mathrm{i}\theta_j(t)}, \tag{5}$$

where $\mathrm{i} = \sqrt{-1}$, e is Euler's number and $\psi(t) = \langle\theta(t)\rangle$ denotes the average phase of the system under the evolution of time t.

To modify the values of $\mathcal{F}$ and r of G, we first define the following procedures:

$$C(e_{ij}) := \text{cut the edge between nodes } i \text{ and } j,$$
$$A(\sigma_{uv}) := \text{add an edge between nodes } u \text{ and } v,$$

where σ_{uv} means that there is no direct connection between nodes $u \in N$ and $v \in N$, i.e., $e_{ij} \in E$ and $\sigma_{uv} \notin E$. Further, letting

$$C(e_{ij}, e_{uv}) := C(e_{ij}) \text{ and } C(e_{uv}),$$
$$A(\sigma_{iu}, \sigma_{jv}) := A(\sigma_{iu}) \text{ and } A(\sigma_{jv}),$$

we have the following observations: (1) the average degree $\langle k\rangle$ keeps constant if $C(e_{ij})$ and $A(\sigma_{uv})$ appear in a pair; (2) the node degree distribution keeps unchanged if $C(e_{ij}, e_{uv})$ and $A(\sigma_{iu}, \sigma_{jv})$ appear in a pair; and (3) r keeps constant if $k_i = k_v$ or/and $k_j = k_u$ under the condition of observation (2). Note that both e_{ij} and e_{uv} are randomly selected from G in this paper. Also, for convenience of description, we define the goal function $\xi^{\delta}(g)$ based on the cut-add strategy, i.e., $C(e_{ij}, e_{uv})$ and $A(\sigma_{iu}, \sigma_{jv})$ appear in a pair, where g is the metric associated with a certain property of G, like r or $\mathcal{F}$, and δ is a symbol corresponding to either the enhancement $(+)$ or the reduction $(-)$ of g. Moreover we employ $\xi^{\delta}(g|c_g)$ to represent the evolution of $\xi^{\delta}(g)$ under the condition of c_g. For example, $\xi^{+}(\mathcal{F}_0|r \equiv r_0)$ means that the robustness $\mathcal{F}$ of G is enhanced to $\mathcal{F}_0$, while its assortativity r is fixed to r_0, where both $\mathcal{F}_0$ and r_0 are given values. In addition, when we specify a certain value, e.g., $r = 0.000$, it means that the difference between the given value and the real value is within 1×10^{-5}. For this case, we use $\xi^{\delta}(g)$ instead of $\xi^{+}(g)$ or $\xi^{-}(g)$ because both of them are employed to adjust the network in a small region around the given value. In other words, for instance, we first use either $\xi^{+}(r_0)$ or $\xi^{-}(r_0)$ to make the network assortativity close to r_0 and then employ both $\xi^{+}(r_0)$ and $\xi^{-}(r_0)$ to further adjust the network, which finally has $r = r_0 \pm 10^{-5}$.

Specifically, given a certain network and g_0 (assuming $g_0 > g$), one procedure $C(e_{ij}, e_{uv})$ and $A(\sigma_{iu}, \sigma_{jv})$ is accepted if it increases g; otherwise, is ignored. Similarly, when $g_0 < g$, we adopt the exchange $C(e_{ij}, e_{uv})$ and $A(\sigma_{iu}, \sigma_{jv})$ if it decreases g. Then we repeat those two procedures until the desired g_0 is reached, which corresponds to $\xi^{\delta}(g)$. During the process to g_0, we may capture some points (say, g_0'), where g undergoes only an enhancement or a reduction. This case is associated with $\xi^{+}(g_0')$ or $\xi^{-}(g_0')$, respectively. Moreover, if there is no special explanation, we also relate $g_0 > g$ to the enhancement of the attribute g and $g_0 < g$ to the reduction.

III. RESULTS

In this section, we will numerically demonstrate the effects of $\mathcal{F}$ as well as the combinations of $\mathcal{F}$ and r on the system of Eq. (4), in which the natural frequency ω_i of each oscillator is fixed to the associated node degree k_i. In addition, the order parameter $\Re$ [Eq. (5)] is calculated by simulating the system long enough until it is stable using the adaptive Runge-Kutta-Fehlberg method [Fehlberg's 4(5) method] [19] with error tolerance 1×10^{-4}, respectively, for the forward and backward evolutions of the coupling strength $\lambda(\tau) := \lambda_0 + \tau\Delta\lambda, \forall\tau \in [0, L], \tau, L \in \mathbb{N}$, where λ_0, $\Delta\lambda$, and L are given values. In other words, each $\lambda(\tau)$ corresponds to a steady state of $\Re(\lambda(\tau))$, and the forward transition of $\Re$ evolves with an ascending order of τ and the backward process with a descending order of τ. Note that in this paper $\Delta\lambda = 0.02$ is considered for each simulation, and all of the initial scale-free (SF) networks are constructed using the Barabási-Albert (BA) model [20]. Also, for convenient description, the symbols e and b are accordingly used to be associated with the forward and backward evolutions of λ.

We first investigate the effects of network robustness $\mathcal{F}$ and assortativity r on ES through $\xi^{\delta}(\mathcal{F})$ and $\xi^{\delta}(r)$ on the network with $\langle k\rangle = 6.0$, respectively. Figure 1(a) shows the order parameter $\Re$ in dependence on the coupling strength λ for the forward and backward synchronization on the initial SF network. The special regions $\mathcal{J}_e$, $\mathcal{J}_b$, and $\mathcal{S}$ mean the following: $\mathcal{J}_e = \Re_e(\lambda(\tau_e + 1)) - \Re_e(\lambda(\tau_e))$ and $\mathcal{J}_b = \Re_b(\lambda(\tau_b)) - \Re_b(\lambda(\tau_b - 1))$ accordingly correspond to the maximal jump size of $\Re$ of the forward and backward synchronization, where $\tau_e := \arg\max_\tau [\Re_e(\lambda(\tau + 1)) - \Re_e(\lambda(\tau))]$ and $\tau_b := \arg\max_\tau [\Re_b(\lambda(\tau)) - \Re_b(\lambda(\tau - 1))]$, and

$$\mathcal{S} = \Delta\lambda \sum_{\tau'=\tau_b}^{\tau_e} [\Re_b(\lambda(\tau')) - \Re_e(\lambda(\tau'))] \tag{6}$$

denotes the hysteresis area, in which $\tau' \in \mathbb{N}$. Indeed [see the red circle in Figs. 1(b)–1(d)], on the one hand, both $\mathcal{S}$ and $\mathcal{J}$ vary over the network assortativity and are suppressed by large

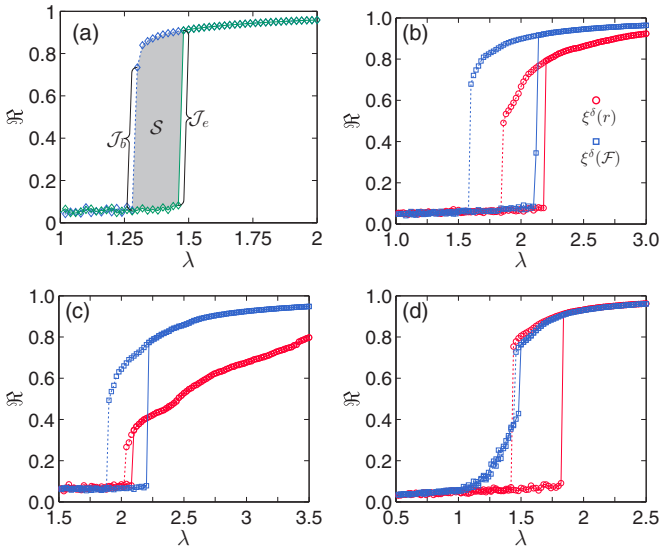

FIG. 1. The magnitude of synchronization $\Re$ versus the coupling strength λ for the forward and backward transitions in networks with $n = 10^3$ and $\langle k\rangle = 6.0$. (a) The initial SF network constructed using the BA model with $\mathcal{F} = 0.197$ and $r = -0.067$. The solid and dashed lines, respectively, correspond to the forward and backward transitions, and between them is the hysteresis area represented by $\mathcal{S}$. Also, the maximal jump sizes of them are denoted by $\mathcal{J}_e$ and $\mathcal{J}_b$, accordingly. (b) $r = 0.000$ with $\mathcal{F} = 0.278$ adjusted by $\xi^\delta(r)$ (red circle) and $\mathcal{F} = 0.250$ with $r = -0.033$ through $\xi^\delta(\mathcal{F})$ (blue square) on the initial SF network. (c) $r = 0.050$ with $\mathcal{F} = 0.354$ and $\mathcal{F} = 0.300$ with $r = -0.006$. (d) $r = -0.050$ with $\mathcal{F} = 0.213$ and $\mathcal{F} = 0.150$ with $r = -0.077$.

or small r, which agrees with the results in Refs. [13,14]. On the other hand, a similar change of $\mathcal{S}$ and $\mathcal{J}$ can be achieved through the adjustment of network robustness [see the blue square in Figs. 1(b)–1(d)], which indicates that there is a range of $\mathcal{F}$ within which $\mathcal{S}$ and $\mathcal{J}$ reach larger values. But, in general, no matter which one between r and $\mathcal{F}$ we adjust, the other one will positively increase or decrease.

Thus, we next fix either $\mathcal{F}$ or r and vary the other one to further verify the dependence of ES on the network robustness and assortativity. Figure 2 illustrates the forward and backward synchronization on networks with different r under three values of $\mathcal{F}$, 0.100, 0.200, and 0.350. Note that $\xi^\delta(r|\xi^\delta(\mathcal{F}))$ means that we first enhance or weaken the network robustness $\mathcal{F}$ and then adjust the network assortativity r to a certain value by keeping $\mathcal{F}$ constant. As manifested in Figs. 2(a)–2(d), though r can narrow the hysteresis area $\mathcal{S}$ and decrease the jump size $\mathcal{J}$, both $\mathcal{S}$ and $\mathcal{J}$ still exist, even r taking a much larger or smaller value (0.150 and -0.200) when $\mathcal{F} = 0.200$. In contrast [Figs. 2(e)–2(h)], the change of $\mathcal{F}$ sharply decreases the size of $\mathcal{S}$ and $\mathcal{J}$, and in some cases they even disappear, which indicates that we can control $\mathcal{S}$ and $\mathcal{J}$ through the interaction of r and $\mathcal{F}$.

In Fig. 3 we show the results of the impacts of the interaction of the network assortativity and robustness on the jump size and hysteresis area of ES, as well as $\mathcal{F}$ of r with $\xi^\delta(r)$ and r of $\mathcal{F}$ with $\xi^\delta(\mathcal{F})$. Without loss of generality, we also consider the cases of SF networks with $n = 10^3$ and $\langle k\rangle = 6.0$. Due to the limitation of n, networks constructed by the BA model are a little disassortative, and their $\mathcal{F}$ is slightly less than 0.200. Therefore, we employ $\xi^\delta(r|\xi^\delta(\mathcal{F}) \equiv 0.200)$ to reconstruct the paradigmatic SF networks to generate our experimental networks. As a result, all networks used for further study in this simulation are with $\langle k\rangle = 6.0$, $\mathcal{F} = 0.200$, and $r = 0.000$ (the differences of both $\mathcal{F}$ and r among those networks are within 1×10^{-5}). Finally, based on those networks, we derive Fig. 3 through $\xi^\delta(r|\xi^\delta(\mathcal{F}))$, which means that $\xi^\delta(\mathcal{F})$ and $\xi^\delta(r|\mathcal{F})$ are successively used to adjust the network structure.

From Fig. 3 we infer the following conclusions: (1) the explosive synchronization is more likely in assortative networks with an enhancement of robustness compared to those with disassortativity and weak robustness; (2) extreme values of r and/or $\mathcal{F}$ will refrain the jump size $\mathcal{J}$ and hysteresis area $\mathcal{S}$; (3) the existence range of $\mathcal{J}$ is much larger than that of $\mathcal{S}$; (4) $\mathcal{J}_e$ is larger than $\mathcal{J}_b$ in assortativity networks, but smaller in disassortativity networks; and (5) there is an area within which both $\mathcal{J}$ and $\mathcal{S}$ reach peaks under the interaction of r and $\mathcal{F}$.

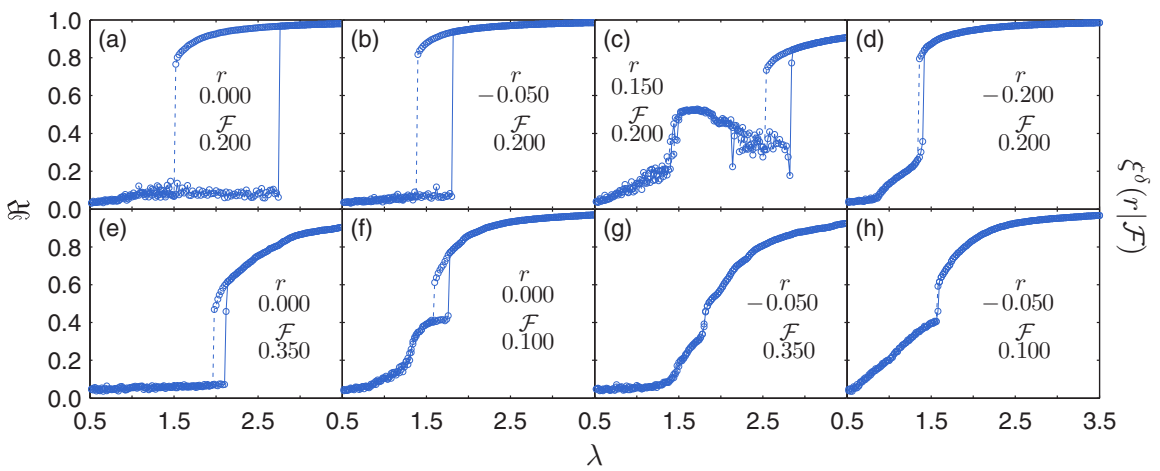

FIG. 2. The magnitude of synchronization $\Re$ versus the coupling strength λ for forward and backward transition on networks with $n = 10^3$ and $\langle k\rangle = 6.0$ under different assortativity r and robustness $\mathcal{F}$. (a–d) $\xi^\delta(r|\xi^\delta(\mathcal{F}) \equiv 0.20)$. (e, g) $\xi^\delta(r|\xi^\delta(\mathcal{F}) \equiv 0.35)$. (f, h) $\xi^\delta(r|\xi^\delta(\mathcal{F}) \equiv 0.10)$.

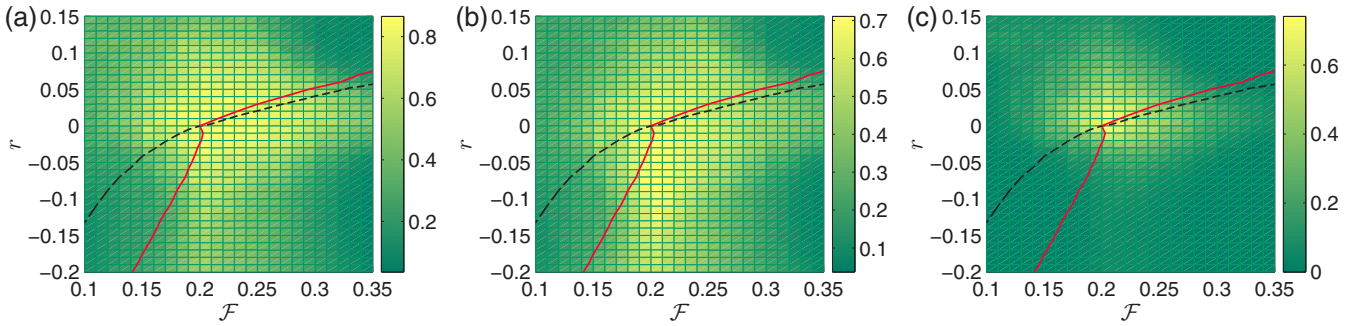

FIG. 3. The jump size J and hysteresis area $\mathcal{S}$ of the network robustness $\mathcal{F}$ and assortativity r. (a) The forward synchronization $\mathcal{J}_e$. (b) The backward synchronization $\mathcal{J}_b$. (c) $\mathcal{S}$. The solid and dashed curves correspond to $\mathcal{F}$ of r with $\xi^\delta(r)$ and r of $\mathcal{F}$ with $\xi^\delta(\mathcal{F})$, respectively. Each result is the average of 20 network realizations.

In detail, the solid curve in Fig. 3 represents the influence of r on $\mathcal{J}$ and $\mathcal{S}$ without the control of $\mathcal{F}$, which is related to Refs. [13–15]. In addition, $\mathcal{F}$ shoots up with the increase of r for $r > 0$, but slowly falls when r decreases if $r < 0$. This means that $\mathcal{J}$ actually remains in the similar range of assortativity and disassortativity if $\mathcal{F}$ is unfixed. With respect to $\mathcal{S}$, we have similar results to Ref. [14], namely, $\mathcal{S}$ reaches its maximum in weak assortativity networks and vanishes quickly as networks become disassortative. A contrary trend of r is observed in the process of $\xi^\delta(\mathcal{F})$ (see the dashed lines in Fig. 3), under which $\mathcal{J}$ and $\mathcal{S}$ disappear dramatically with the decrease of $\mathcal{F}$ and stay in a large range of increasing $\mathcal{F}$.

We further validate the above conclusions in a much larger network with $n = 10^4$ and $\langle k \rangle = 6.0$. Figs. 4(b), 4(i), and 4(j) and Figs. 4(b)–4(d), 4(k), and 4(l) show how ES is influenced by varying $\mathcal{F}$ or r, while the other one is fixed: making a network fragile is more likely to collapse ES than enhancing the network's robustness, and a larger $\mathcal{S}$ can be observed in assortative networks compared to disassortative networks. When r is not fixed [Figs. 4(e) and 4(f)], $\mathcal{J}$ and $\mathcal{S}$ disappear in a high speed with decreasing $\mathcal{F}$ and stay in a large range for increasing $\mathcal{F}$. Moreover, in these cases, $\mathcal{S} = 1.979$ reaches its maximum when $r = 0.000$ and $\mathcal{F} = 0.200$, and it is also much larger than that in the network with $n = 10^3$.

IV. DISCUSSION

By now, we have presented our results of $\xi^\delta(r|\xi^\delta(\mathcal{F}) \equiv \mathcal{F}_0)$, namely, the network robustness $\mathcal{F}$ is initially given for a certain value $\mathcal{F}_0$, and then the network assortativity is further adjusted with the constraint $\mathcal{F} \equiv \mathcal{F}_0$. But what would happen when we use $\xi^\delta(\mathcal{F}|\xi^\delta(r) \equiv r_0)$ to modify the network? Figure 5 shows the corresponding results of $\xi^\delta(\mathcal{F}|\xi^\delta(r))$ on the same network as in Fig. 2. The strongest difference between them is in Fig. 2 and Figs. 5(c), 5(d), 5(g), and 5(h), where the hysteresis area vanishes in one network, while it

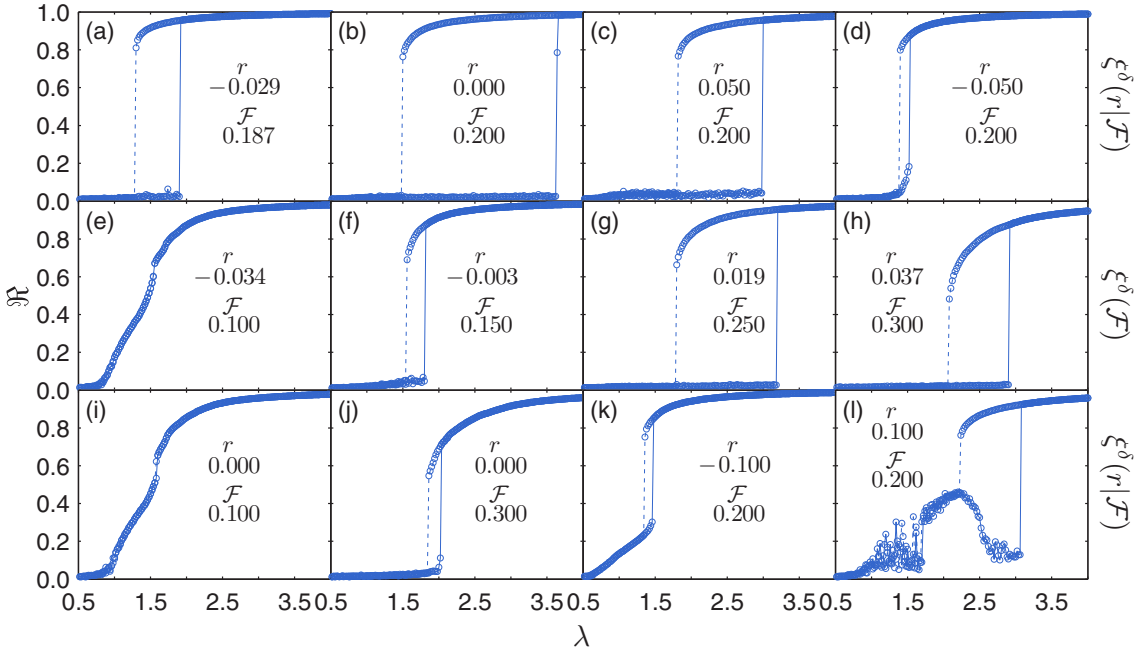

FIG. 4. The magnitude of synchronization $\Re$ versus the coupling strength λ for forward and backward transition on networks with $n = 10^4$ and $\langle k \rangle = 6.0$ for different r and $\mathcal{F}$. The result of the paradigm network from the BA model is reported in panel (a).

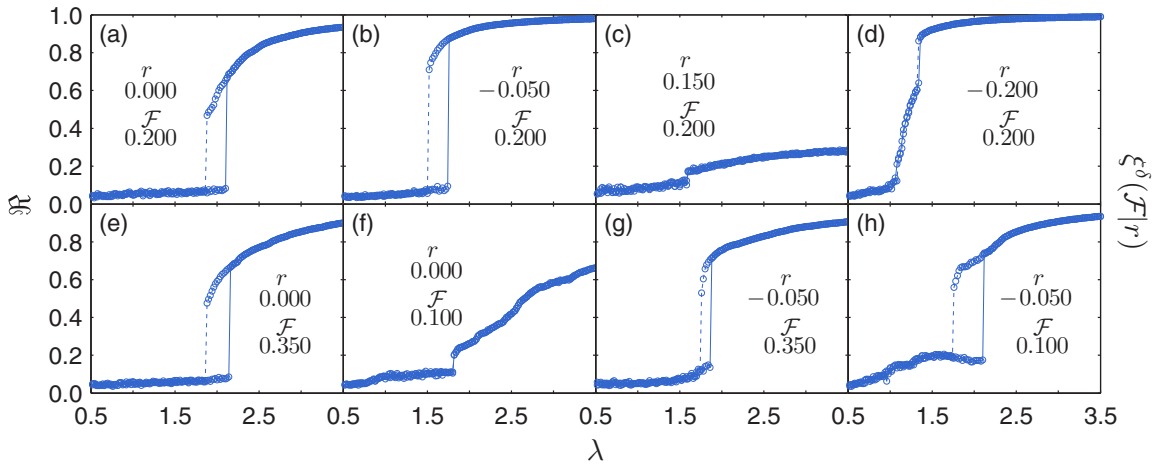

FIG. 5. The magnitude of synchronization $\Re$ versus the coupling strength λ for forward and backward transition on networks with $n = 10^3$ and $\langle k\rangle = 6.0$ under different assortativity r and robustness $\mathcal{F}$. (a, e, f) $\xi^\delta(\mathcal{F}|\xi^\delta(r) \equiv 0.000)$. (b, g, h) $\xi^\delta(\mathcal{F}|\xi^\delta(r) \equiv -0.050)$. (c) $\xi^\delta(\mathcal{F}|\xi^\delta(r) \equiv +0.150)$. (d) $\xi^\delta(\mathcal{F}|\xi^\delta(r) \equiv -0.200)$.

still exists in the corresponding other one, even though they both have the same r and $\mathcal{F}$. One reason may be ascribed to the fact that both r and $\mathcal{F}$ are disturbed heavily in Figs. 2(g) and 2(h) and Figs. 5(c) and 5(d); e.g., for Fig. 5(c), $\mathcal{F}$ will considerably increase with the rise of r and then be dragged back to 0.200 (also see the solid line in Fig. 3). This can be verified in a similar way as in Fig. 3.

Another interesting difference is that the hysteresis area in Fig. 2(a) is much larger than that in Fig. 5(a) (also see Fig. 8 below). The main distinct process between them is that in the change trend of $\mathcal{F}$, i.e., for $\xi^\delta(r|\xi^\delta(\mathcal{F}))$ [Fig. 2(a)], $\mathcal{F}$ undergoes only an increasing process (ignore the tiny adjustment), while it first increases with the rise of r and then decreases to 0.200 through $\xi^\delta(\xi^\delta(\mathcal{F})|r)$ [Fig. 5(a)]. Thus, how do the increasing and decreasing behaviors influence the ES? Figure 6 shows $\mathcal{S}$ of the perturbations of r and $\mathcal{F}$. For a convenient description, we employ $r(P_t)$ and $\mathcal{F}(P_t)$ to be associated with the perturbation step P_t. In detail, at each step (P_t), the associated property (r and/or $\mathcal{F}$) is either increased $[\xi^+(g)]$ or decreased $[\xi^-(g)]$ (assuming 10^4 times of the cut-add strategy), and then adjusted back to the given value, i.e., networks for each data point have similar properties. Also, we here set odd steps ($P_t = 1, 3, \ldots$) as the decreasing process and even steps ($P_t = 2, 4, \ldots$) as the increasing process. Considering Fig. 6(e) as an example, we first employ $\xi^-(r)$ (10^4 times of the cut-add strategy) to reduce the network assortativity and then adjust it to $r(1) \approx r(0)$ through $\xi^\delta(r)$ to obtain the network for $P_t = 1$. Based on this network, we further use $\xi^+(r)$ to enhance the network assortativity and then tune it back to $r(2) \approx r(1) \approx r(0)$ to get the network for $P_t = 2$, etc. In this manner, we continually disturb r but at each data point $r(P_t) \approx r(0)$, $P_t = 1, 2, 3 \ldots$.

As shown in Figs. 6(a)–6(d), the hysteresis area $\mathcal{S}$ decreases with the increase of P_t if we disturb the network assortativity when keeping $\mathcal{F}$ constant, and it undergoes a slight fluctuation by $\xi^\delta(\mathcal{F}|r)$. Note that the perturbation

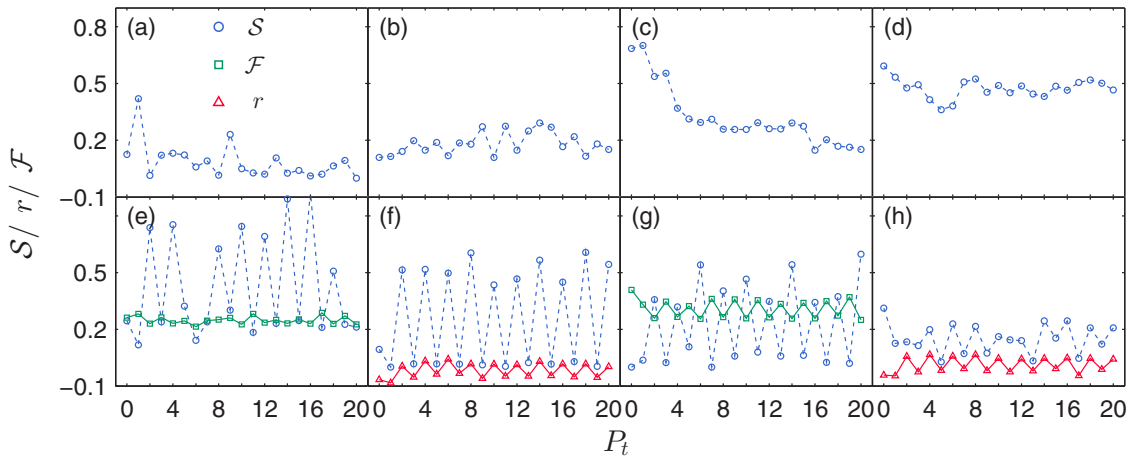

FIG. 6. The hysteresis area $\mathcal{S}$ versus the perturbations of network assortativity r and robustness $\mathcal{F}$ on networks with $\langle k\rangle = 6.0$, $n = 10^3$ (the same initial network as Fig. 2) for (a, b, e–h) and $n = 10^4$ (the same initial network as in Fig. 4) for (c, d). (a, b) Respectively for $\xi^\delta(r|\mathcal{F})$ and $\xi^\delta(\mathcal{F}|r)$ with $r(0) = -0.067$ and $\mathcal{F}(0) = 0.197$. (c, d) Respectively for $\xi^\delta(r|\mathcal{F})$ and $\xi^\delta(\mathcal{F}|r)$ with $r(0) = -0.029$ and $\mathcal{F}(0) = 0.187$. (e, g) $\xi^\delta(r)$ with $r(0) = 0.000$ and $r(0) = 0.050$, accordingly. (f, h) $\xi^\delta(\mathcal{F})$ with $\mathcal{F}(0) = 0.197$ and $\mathcal{F}(0) = 0.250$, accordingly.

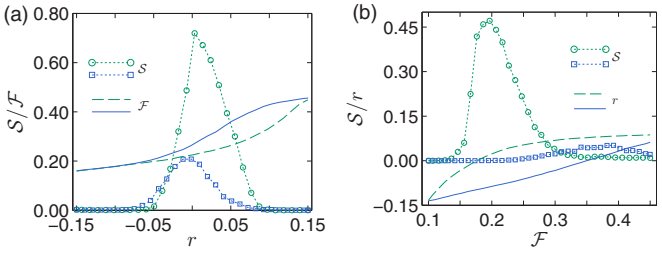

FIG. 7. The hysteresis area $\mathcal{S}$ and the network robustness $\mathcal{F}$ or assortativity r versus r or $\mathcal{F}$ for forward (blue) and backward (green) evolutions on networks with $\langle k\rangle = 6.0$ and $n = 10^3$.

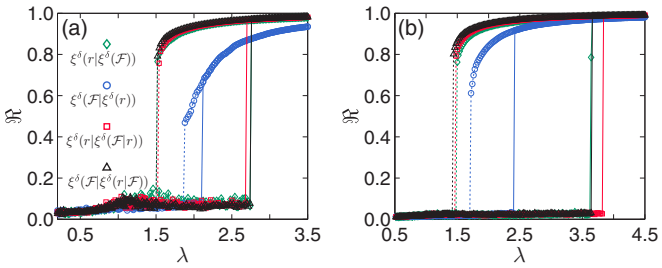

FIG. 8. The magnitude of synchronization $\Re$ versus the coupling strength λ for forward and backward transition on networks with $\langle k\rangle = 6.0$, $r = 0.000$ and $\mathcal{F} = 0.200$ for (a) $n = 10^3$ and (b) $n = 10^4$. $\xi^\delta(r|\xi^\delta(\mathcal{F}|r))$ here means that $\mathcal{F}$ is first adjusted to 0.200 by keeping r constant and then change r to 0.000 with fixed $\mathcal{F} \equiv 0.200$.

process is different from that in Fig. 3. Also, we might focus the utmost interest on Figs. 6(e)–6(h), where we consider only the perturbation from either r or $\mathcal{F}$. For both cases, $\mathcal{S}$ periodically fluctuates in the evolution of P_t. Specifically, when disturbing r, $\mathcal{S}$ negatively changes as the network robustness evolves, while it is positively correlated to r through $\xi^\delta(\mathcal{F})$. In addition, the fluctuation between two adjacent P_t is very large. This suggests that quite different $\mathcal{S}$ will be obtained even though two networks have almost similar r or $\mathcal{F}$.

To further demonstrate the results of Figs. 6(e)–6(h), we show the hysteresis area $\mathcal{S}$ and the network robustness $\mathcal{F}$ (or assortativity r) against the forward and backward evolutions of r (or $\mathcal{F}$) in Fig. 7. For the backward evolution of r [Fig. 7(a)], we first disturb r through $\xi^\delta(r)$ until the network reaches a stable state (assuming $P_t \in [1, 100]$), where $\lfloor 10\,000/P_t \rfloor$ is conducted for the cut-add strategy at each perturbation step. After this, r is increased to 0.15 and then gradually decreased to -0.15, during which we capture the temporary networks with an interval of around 0.01 of r. We independently repeat this process 20 times and obtain the backward transition of r, which is shown as the green-dotted-circle curve in Fig. 7(a). The forward evolution of r is gathered in a similar way but with the process that r is decreased to -0.15 and then gradually increased to 0.15. The similar strategy is also conducted to evolve $\mathcal{F}$.

As illustrated in Fig. 7, there is a gap of $\mathcal{F}$ or r between $\xi^-(\cdot)$ and $\xi^+(\cdot)$. This gap changes the place of the peak of $\mathcal{S}$, which indicates that δ of $\xi^\delta(\cdot)$ truly plays an important role in $\mathcal{S}$. Moreover, the magnitude of synchronization $\Re$ versus the coupling strength λ for the forward and backward transitions on networks with the same $\langle k\rangle$, r and $\mathcal{F}$ is demonstrated in Fig. 8. These results are also twofold. On the one hand, there might be a maximum of $\mathcal{S}$ achieved by appropriate adjustments of r and $\mathcal{F}$. On the other hand, the order of the adjustment plays quite a vital role, which means that r and $\mathcal{F}$ are not the only two properties influencing ES. By and large, this problem is still open and needs further research.

V. CONCLUSION

The robustness of networks as a fundamental problem in network science has been widely studied during the past decade [17]. Those studies mainly consider how the structure of networks influences their robustness. In this paper, we view the network robustness $\mathcal{F}$ as a property of networks and use it to capture the change of networks' structure. More specifically, we have numerically studied effects of the network robustness as well as its interaction with network assortativity r on explosive synchronization and have found that both extreme values of $\mathcal{F}$ and r would suppress ES, especially the hysteresis area between the forward and backward transitions. In particular, for a network constructed by the BA model, there is a maximum of hysteresis area achieved by appropriate adjustments of $\mathcal{F}$ and r. In addition, our discussion reveals that the change trends of both the network robustness and assortativity play important roles on ES. In other words, different behaviors of ES are found in networks with similar $\mathcal{F}$ and/or r if the networks undergo different change processes, which leaves the problem of effects of the network structure on ES still partly open.

ACKNOWLEDGMENTS

We would like to thank Y. Zou, F. Hellmann, P. Schultz and C.M. Zheng for useful discussions. This work was supported in part by the High Performance Computer System at the Potsdam Institute for Climate Impact Research through the European Regional Development Fund, the German Federal Ministry of Education and Research and the Land Brandenburg, in part by the China Scholarship Council Scholarship, and in part by Deutsche Forschungsgemeinschaft/Fundação de Amparo à Pesquisa do Estado de São Paulo (DFG/FAPESP) under Grant IRTG 1740/TRP 2015/50122-0.

[1] S. Boccaletti, V. Latora, Y. Moreno, M. Chavez, and D.-U. Hwang, Phys. Rep. **424**, 175 (2006).
[2] P. J. Menck, J. Heitzig, J. Kurths, and H. J. Schellnhuber, Nat. Commun. **5**, 3969 (2014).
[3] D. Brockmann and D. Helbing, Science **342**, 1337 (2013).
[4] C. M. Schneider, A. A. Moreira, J. S. Andrade, S. Havlin, and H. J. Herrmann, Proc. Natl. Acad. Sci. USA **108**, 3838 (2011).
[5] G. F. Chami, S. E. Ahnert, N. B. Kabatereine, and E. M. Tukahebwa, Proc. Natl. Acad. Sci. USA **114**, E7425 (2017).
[6] A. Arenas, A. Díaz-Guilera, J. Kurths, Y. Moreno, and C. Zhou, Phys. Rep. **469**, 93 (2008).

[7] F. A. Rodrigues, T. K. D. Peron, P. Ji, and J. Kurths, Phys. Rep. **610**, 1 (2016).
[8] J. Gómez-Gardenes, S. Gómez, A. Arenas, and Y. Moreno, Phys. Rev. Lett. **106**, 128701 (2011).
[9] P. Ji, T. K. DM. Peron, P. J. Menck, F. A. Rodrigues, and J. Kurths, Phys. Rev. Lett. **110**, 218701 (2013).
[10] Y. Zou, T. Pereira, M. Small, Z. Liu, and J. Kurths, Phys. Rev. Lett. **112**, 114102 (2014).
[11] Y. Kuramoto, in *International Symposium on Mathematical Problems in Theoretical Physics* (Springer, Kyoto/Japan, 1975), pp. 420–422.
[12] L. Zhu, L. Tian, and D. Shi, Phys. Rev. E **88**, 042921 (2013).
[13] P. Li, K. Zhang, X. Xu, J. Zhang, and M. Small, Phys. Rev. E **87**, 042803 (2013).
[14] I. Sendiña-Nadal, I. Leyva, A. Navas, J. Villacorta-Atienza, J. A. Almendral, Z. Wang, and S. Boccaletti, Phys. Rev. E **91**, 032811 (2015).
[15] T. K. DM. Peron, P. Ji, F. A. Rodrigues, and J. Kurths, Phys. Rev. E **91**, 052805 (2015).
[16] M. E. J. Newman, Phys. Rev. Lett. **89**, 208701 (2002).
[17] A.-L. Barabási *et al.*, *Network Science* (Cambridge University Press, Cambridge, 2016).
[18] R. Cohen, K. Erez, D. Ben-Avraham, and S. Havlin, Phys. Rev. Lett. **86**, 3682 (2001).
[19] E. Fehlberg, Low-order classical runge-kutta formulas with stepsize control and their application to some heat transfer problems, Technical Report No. NASA-TR-R-315 (NASA, Washington, D. C., 1969).
[20] A.-L. Barabási and R. Albert, Science **286**, 509 (1999).